Propagation Delay Based Positioning Using IEEE 802.11b Signals

Golaleh Rahmatollahi[a], Stefan Galler[b], Jens Schroeder[c], Klaus Jobmann[d], Kyandoghere Kyamakya[e]

[a]IKT, Hannover, Germany, e-mail: gola@ant.uni-hannover.de
[b]IKT, Hannover, Germany, e-mail: stefan.galler@ant.uni-hannover.de
[c]IKT, Hannover, Germany, e-mail: jens.schroeder@ant.uni-hannover.de
[d]IKT, Hannover, Germany, e-mail: jo@ant.uni-hannover.de
[e]ISYS, Klagenfurt, Austria, e-mail: kyamakya@isys.uni-klu.ac.at

Abstract - In contrast to most WLAN localization approaches in literature, which are based on received signal strength indicator (RSSI), we examine the location capabilities of signal propagation delay measurements. We use IEEE 802.11b throughout this paper, as it has become the most common WLAN standard.
Signal propagation delays are determined by direct sampling of RF-signals captured by WLAN antennas and subsequent cross-correlation and interpolation. The functionality of the system is evaluated by wired measurements and in an anechoic chamber. In addition, a real world measurement campaign performed in an indoor environment will be presented.

1 Introduction

WLAN gained widespread acceptance over the past decade and yielded a large number of wireless applications. In response to this growth, a demand for local positioning systems has arisen, as the combination of individual positioning information and mobile communication enables a variety of new Location-Based-Services (LBS) [1]. Hence, the investigations throughout this paper will analayze the suitability of IEEE 802.11b signals for localization issues and will give an estimate of the feasible positioning accuracy using the cross-correlation method to determine propagation delays of IEEE 802.11b signals.
Section 2 presents the system architecture including the signal processing steps to determine signal propagation delays. Section 3 deals with the wired reference system and describes the necessity of an interpolation algorithm for WLAN signals. Additionally, measurements carried out in an anechoic chamber are presented. Finally, section 4 discusses the measurements of an indoor environment including one dimensional distance determinations and three dimensional positioning.

2 System Architecture

2.1 System Setup

The measurement system consists of a mobile WLAN unit, four stationary antennas connected to a digital sampling oscilloscope, and a signal processing PC (see Fig. 1). RF-signals emitted by the mobile unit are captured by the antennas and directly sampled by the oscilloscope at 10 GHz sample frequency. The raw measurement data is transferred from the digital sampling

oscilloscope to the signal processing PC running MATLAB. Using correlation methods, the propagation delay differences of all antennas are estimated. The four antennas serve as reference points with known positions to allow three dimensional time difference of arrival (TDOA) localization of the mobile unit. Because of its good auto-correlation properties, we use the IEEE 802.11b physical layer convergence protocol (PLCP) preamble as measurement signal.

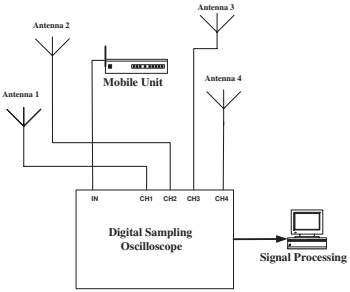

Figure 1: System Setup

2.2 Propagation Delay Based Positioning

In order to estimate the mobile device's position, two main processing steps have to be performed. The first step consists of finding the time of arrival differences and resulting differences in distance by estimating the maximum of the cross-correlation function [2]

$$\Delta t_{ij} = t_i - t_j = argmax_\tau \int s_j(t) s_i(t+\tau) dt, 1 \leq i < j \leq N, \tag{1}$$

where t_i and t_j denote the absolute times of arrival at base station i and j, respectively. N represents the number of base stations.
The TDOA estimations Δt_{ij} are converted to range differences Δd_{ij} through multiplication by the speed of light c:

$$\Delta d_{ij} = c\Delta t_{ij} = c(t_i - t_j) = d_i - d_j. \tag{2}$$

The second step is to use this data and the known reference positions $[x_i, y_i, z_i]^T$ of the four antennas to calculate the current mobile unit's position $x = [x, y, z]^T$:

$$d_i = \|\mathbf{x} - \mathbf{x_i}\| = \sqrt{(\mathbf{x} - \mathbf{x_i})^2 + (\mathbf{y} - \mathbf{y_i})^2 + (\mathbf{z} - \mathbf{z_i})^2}. \tag{3}$$

To solve this set of non-linear equations, Bancroft's algorithm is applied [3].

2.3 802.11b PLCP Preample

As stated, the PLCP preamble of IEEE 802.11b is used as measurement signal. The DBPSK modulated spread WLAN signal is first filtered by a raised cosine filter before being transmitted at 2.4 GHz carrier frequency. The bandwidth of the WLAN signal corresponds to 22 MHz due to the chip rate of 11 MHz. The envelope of the signal shown in Fig. 2 (a) corresponds to the baseband signal and shows the Barker sequence applied for spreading. Due to the raised cosine filter, the signal has a sinc-like shape. The grey box indicates the zoomed area shown in Fig. 2 (b) which depicts the high frequent carrier at 2.4 GHz visible between the envelope. As the sample frequency is roughly four times higher than the carrier frequency, one sinus period of the carrier frequency contains four samples. Due to the ratio of sample frequency to carrier frequency, which is not a multiple of 2π, the shape of the sampled signal shows corrugations (see Fig. 2 (b)).

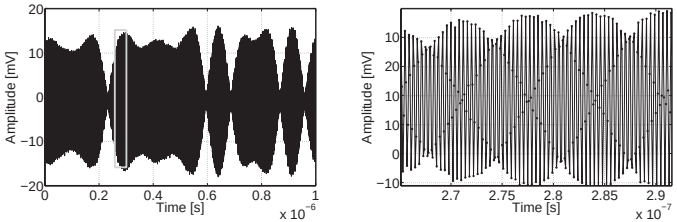

(a) (b)

Figure 2: (a) WLAN Oscilloscope Signal, (b) Zoom into Signal

In order to estimate the signal propagation delays, the four oscilloscope channels are cross-correlated, yielding six correlation maxima. Figure 3 (a) exemplarily shows the cross-correlation function of two measured channels.
The structure of the correlation is determined by the applied Barker code. Hence, referring to the side lobes the main peak is distinctive due to the good correlation properties of the Barker code. When zooming into the main peak, the relative broadness of the correlation maximum becomes obvious (see Fig.3 (b)). The narrowband WLAN signal of 22 MHz yields a relatively broad maximum and complicates the signal propagtion delay estimations, as disturbances due to noise effects can easily cause estimation errors. Figure 3 (c) shows a second zoom into the maximum peak showing the correlation maximum in detail. It has the same corrugated structure as the WLAN signal shown in figure 2 (b) due to the effects of sampling.

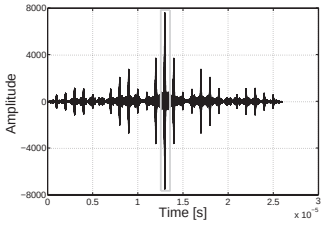

(a)

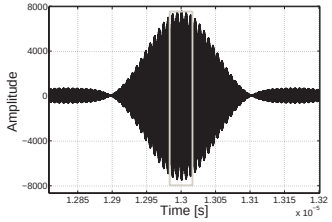

(b)

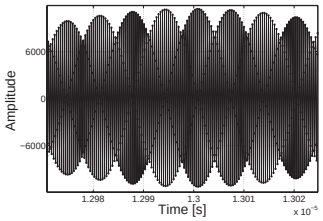

(c)

Figure 3: (a) Cross-Correlation of Two Channels, (b) Zoom into Peak, (c) Zoom into (b)

3 Reference System and Anechoic Chamber

The basic functionality of the system was first evaluated by wired measurements, indicating the need for an interpolation algorithm. In the following, system functionality was confirmed in an anechoic chamber.

3.1 Reference System and Interpolation

As the mobile unit is connected to all four channels of the oscilloscope by wires, noise level and radio propagation channel effects are negligible. 20 measurements were preformed without changing the system's setup. Only time of arrival differences were evaluated, as position determination is not applicable. We expect constant signal propagation delays of zero for this case, as the system setup is symmetrical including cables of approximately same lengths. Fig. 4 exemplarily shows the propagation delay differences measured between two channels.
Obviously, the obtained results are neither constant nor zero. Thus, we must assume a signal processing error which has to be analyzed by further investigations. The error occuring during the reference system measurements has its seeds in the effects of sampling as described in section 2.3. Due to the small length differences of the used cables, the signals are displaced in the order of sub samples, which is not determinable by the conventional correlation method, as it can only resolve complete samples. Computer simulations of an IEEE 802.11b signal show that the ratio of sample frequency to carrier frequency, if not a multiple of 2π, yields the obtained offset errors.
The cross-correlation technique was applied to two simulated WLAN signals. One signal was

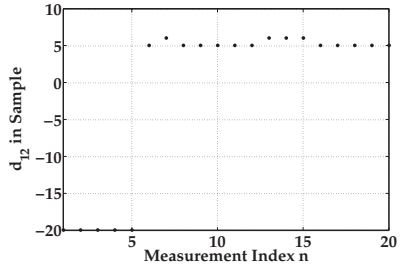

Figure 4: Signal Propagation Delay between two Channels without Interpolation

gradually displaced in sub sample steps and the cross-correlation maximum was determined. Considering the relation between sample frequency f_s and carrier frequency f_0 which was set to approximately $\frac{f_s}{f_0} = \frac{10GHz}{2.414GHz} \approx \frac{29}{7}$ to simulate the real values. The following equation shows what occurs for non 2π periodic sampling of a sine wave. The sampling of the analog sinusoidal signal $s(t) = sin(2\pi f_0 t)$ can be described by [4]:

$$s_a(t) = \sum_{n=-\infty}^{\infty} s(nT_s)\delta(t - nT_s) \tag{4}$$

$$s_a(t) = \sum_{n=-\infty}^{\infty} sin(2\pi f_0 nT_s)\delta(t - nT_s) \tag{5}$$

for $T_s = 1/f_s$ equation 5 can be transformed into:

$$s_a(t) = \sum_{n=-\infty}^{\infty} sin(2\pi n\frac{f_0}{f_s})\delta(t - n\frac{1}{f_s}). \tag{6}$$

The term $\frac{f_s}{f_0}$ appears inversely in the described equation and can be expressed by $K = \frac{f_s}{f_0}$ leading to:

$$s_a(t) = \sum_{n=-\infty}^{\infty} sin(2\pi n\frac{1}{K})\delta(t - n\frac{1}{f_s}). \tag{7}$$

$K \approx \frac{29}{7}$ indicates that the sine wave is sampled by a factor which is not a multiple of 2π. Hence, the sampling values do not recur within one 2π period but after the 7th sinus period. Although the Nyquist criterion is fulfilled, this kind of sampling causes errors in the case of simple maximum detection. Table 1 shows the results of the simulations.
The calculated delays first decrease from -4 to -16 in steps of 4 and increase to 13 in the middle of two samples before decreasing again. The results of the sub sample delays between 1 and 4 samples show similar properties but differ in their absolute values.
Using a multiple of 2π to sample the sine wave, the offsets does not occur anymore and the simulations yield expected values.

Delay	Calc. Delay [Sample]
0.0	0
0.1	-4
0.2	-4
0.3	-8
0.4	-12
0.5	17
0.6	13
0.7	9
0.8	5
0.9	5

Table 1: Sub-Sample Delay Determination

One solution to cope with this problem is to approximate the equivalent continous signal by interpolation. In order to minimize the computations only the correlation peak is interpolated. The interpolation algorithm is implemented in two steps. First, the data is upsampled by inserting n zeros leading to an n times higher sampling rate as the original rate. The simulation results yielded a factor of $n = 100$ to completely delete the offsets.
The second step consists of a polyphase filter implementation containing an anti-aliasing lowpass FIR filter with a Kaiser window. The optimal filter length is set to $L = 300$ which was also determined by computer simulations. The measurement results of the reference system including interpolation is shown in figure 5.

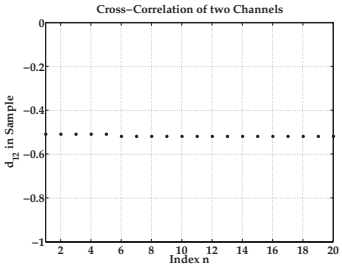

Figure 5: Signal Propagation Delay between two Channels with Interpolation

As it can be seen in 5, measurement variations are in the order of hundredths of one sample, corresponding to length variations of sub mm, which can be regarded as the overall measurement uncernity.

3.2 Anechoic Chamber

As the reference system yielded expected values if an adequate interpolation technique is used, the wireless system's functionality was tested next in an anechoic chamber where antenna effects are present, but multipath propagation effects are still negligible. Due to the chamber's limited extent, only two antennas have been used, hence positioning is restricted to one dimension. Fig. 6 shows the setup of the anechoic chamber measurement system.
Before estimating the signal propagation delays, a calibration of the system has been performed

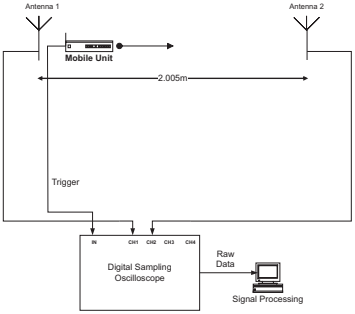

Figure 6: System Setup of Anechoic Chamber

to eliminate additional offsets, as in this setup the antennas are connected to the oscilloscope by wires of different lengths. The mobile unit was moved from antenna 1 to antenna 2 in 18 steps (see Fig. 7).

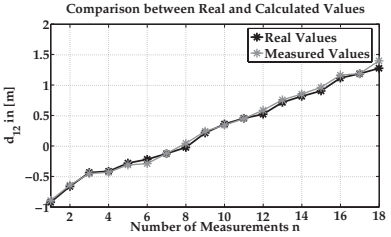

Figure 7: Propagation Delays of Anechoic Chamber

Table 2 shows the preformance metrics of the measurement results of the distance differences d_{12} including the root mean square (RMS) and the standard deviation σ of the error.

RMS [m]	σ **[m]**
0.086	0.045

Table 2: Accuracy Performance in Anechoic Chamber

The obtained measurement error in the anechoic chamber still shows expected results. However, due to practical measurement uncernity as well as antenna and propagation effects, the measurement results are worse in comparence to the wired reference system, but still yield an accuracy performance of 8.6 centimeters.

4 Indoor Measurement Campaign

In order to investigate real world behaviour, a measurement campaign in an indoor environment was carried out. The mobile unit was moved in 10 cm steps along a 9.9 m line parallel to the

x-axis at a constant height. At every position of the mobile unit, line of sight conditions were assured.
First, one dimensional distance measurements were performed using two antennas. A copy of the measurement signal, directly transmitted by wire from the mobile unit to the oscilloscope, served as template to allow time of arrival measurements. Second, three dimensional positioning measurements were carried out. The measurement setup was expanded to a four antenna constellation, as with the implemented time difference of arrival (TDOA) method, four antennas are needed to estimate three dimensional positions. An optimal geometric constellation of the system is achieved for those cases, where the antennas are placed in the corners of a regular tetrahedron [5]. As this constellation is not realistic for our indoor environment, the regular tetrahedron constellation was applicably stretched. The distance differences between the mobile unit and the four antennas were determined by cross-correlation of all four channels. Fig. 4 shows the one dimensional distances between the mobile unit and the antennas and Table 3 the corresponding performance metrics.

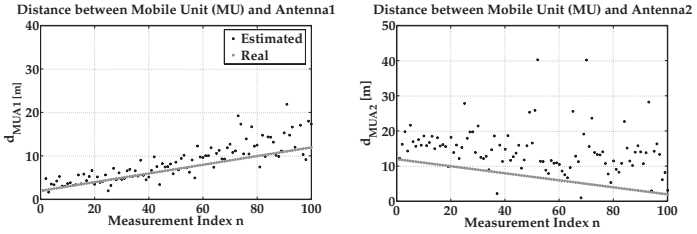

(a) (b)

Figure 8: (a) Distance between mobile unit and antenna 1, (b) Distance between mobile unit and antenna 2

	RMS [m]	σ **[m]**
MU/A1	3.562	1.769
MU/A2	9.879	2.519

Table 3: Accuracy Performance of one dimensional Measurements

Fig. 9 shows the three dimensional positioning results and Table 4 the corresponding accuracy performance.
The one dimensional distance estimations as well as the three dimensional positioning show that multipath propagtions due to the radio channel mainly deteriorate the accuracy. In contrast to the reference system measurements and the anechoic chamber measurements, the results are in the order of 4-12 m.

5 Conclusion

The system architecture, an interpolation algorithm to improve the accuracy, and the measurement results of the IEEE 802.11b positioning system have been described. An analysis of the system's functionality under ideal conditions in terms of a wired reference system and in an anechoic chamber where radio channel effects are negligible, show that the feasible accuracy is in the order of centimeters. However, in real world scenarios where multipath propagation occurs,

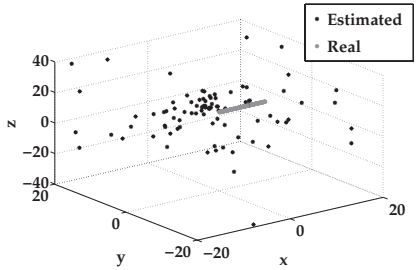

Figure 9: 3 dimensional Positioning

	RMS [m]	σ **[m]**
x	12.157	3.483
y	19.431	4.414
z	22.172	4.654

Table 4: Accuracy Performance of 3 dimensional Positioning

the positioning system using IEEE 802.11b signals in combination with the cross-correlation algorithm shows results in the order of 4-12 m. As the conventional correlation method is able to resolve multiple paths within the chip rate of 11 MHz, corresponding to approximately 27 m, shorter paths cannot be resolved. Hence, so-called Super Resolution techniques could be implemented to resolve shorter paths. Some investigations in [6] show, that an improvement of factor two is feasible if an adequate high resolution algorithm is applied. However, in order to achieve accuracies in the order of sub meters, other wireless technologies must be applied for signal propagation delay estimations.

References

[1] K. Pahlavan, P. Krishnamurthy,"Principles of Wireless Networks", Prentice Hall, New Jersey, 2002

[2] J. Schroeder, S. Galler, K. Kyamakya,"A Low-Cost Experimental Ultra-Wideband Positioning System", presented at IEEE International Conference on Ultra-Wideband, Zurich, 2005

[3] S. Bancroft,"An Algebraic Solution of the GPS Equations,"IEEE Transactions on Aerospace and Electronic Systems, vol. AES-21,pp. 56-59, 1985

[4] A.V. Oppenheim, R.W. Schafer,"Zeitdiskrete Signalverarbeitung", Oldenbourg, München, 1995

[5] B. Yang and J. Scheuing, "Cramer-Rao bound and optimum sensor array for source localization from time differences of arrival " presented at IEEE International Conference on Acoustics, Speech, and Signal Processing (ICASSP), 2005

[6] L.Dumont, M. Fattouche, G. Morrison,"Super-Resolution of Multipath Channels in a Spread Spectrum Location System", Electronics Letters, September 1994.

.